Graph-Based Range Image Registration Combining Geometric and Photometric Features

Ikuko Shimizu[1], Akihiro Sugimoto[2], and Radim Šára[3]

[1] Tokyo University of Agriculture and Technology, Japan
[2] National Institute of Informatics, Japan
[3] Czech Technical University, Czech Republic
ikuko@cc.tuat.ac.jp, sugimoto@nii.ac.jp, sara@cmp.felk.cvut.cz

Abstract. We propose a coarse registration method of range images using both geometric and photometric features. The framework of existing methods using multiple features first defines a single similarity distance summing up each feature based evaluations, and then minimizes the distance between range images for registration. In contrast, we formulate registration as a graph-based optimization problem, where we independently evaluate geometric feature and photometric feature and consider only the order of point-to-point matching quality. We then find as large consistent matching as possible in the sense of the matching-quality order. This is solved as one global combinatorial optimization problem. Our method thus does not require any good initial estimation and, at the same time, guarantees that the global solution is achieved.

1 Introduction

Automatic 3D model acquisition of the real-world object is important for many applications such as CAD/CAM or CG. A range sensor, which is a sensing device directly measuring 3D information of an object surface, is a useful tool in modeling 3D objects. An image of an object captured by a range sensor is called a range image and it provides a partial shape of the object in terms of the 3D coordinates of surface points in which the coordinate system is defined by the position and orientation of the range sensor. To obtain the full shape of an object, therefore, we have to align range images captured from different viewpoints. This alignment, i.e., finding the rigid transformation between coordinate systems that aligns given range images, is called range image registration.

Widely used methods for range image registration are the iterative closest point (ICP) method proposed by [1] and its extensions [2,8,14,16]. These methods iterate two steps: Each point in one range image is transformed by a given transformation to find the closest point in the other range image. These point correspondences are then used to estimate the transformation minimizing matching errors. In order to robustly[1] realize range image registration, some features

[1] The terminology "robust" in this paper means that the possibility of successful registration is enhanced; registration is more successful.

B.K. Ersbøll and K.S. Pedersen (Eds.): SCIA 2007, LNCS 4522, pp. 542–552, 2007.

reducing matching ambiguity are proposed in addition to simply computed geometric features [4,5,6,7,12,13]. They are, for example, color attributes [5], chromaticity [7], normal vectors [4], curvatures themselves and their features [6,12], and attributes representing overlapping areas of planes [13]. Combining different kinds of features enhances robustness for registration; nevertheless, defining one common meaningful metric for similarity using different kinds of features is still even difficult.

On the other hand, a method using a graph-based optimization algorithm for range image registration is proposed [11]. The method formalizes the matching problem as a discrete optimization problem in an oriented graph so that optimal matching becomes equivalent with the uniquely existing maximum strict subkernel (SSK) of the graph. As a result, this method does not require any good initial estimation and, at the same time, guarantees that the global solution is achieved. In addition, it also has an advantage that a part of data is rejected rather than forcefully interpreted if evidence of correspondence is insufficient in the data or if it is ambiguous. The method, however, deals with geometric features only and fails in finding matching for data of an object having insufficient shape features.

In this paper, we extend the graph-based method [11] so that it does work even for the case of data with insufficient shape features. We incorporate the combination of geometric and photometric features into the framework to enhance the robustness of registration. Existing methods [4,5,6,7,12,13] combining such features define a single metric by adding or multiplying similarity criteria computed from each feature to find point matches. In contrast, our proposed method first evaluates each point match independently using each feature, and then determines the order of matching quality among all possible matches. To be more concrete, for two point-matches, if similarity of one match is greater than the other over all features, we regard that the former is strictly superior to the latter. Otherwise, we leave the order between the two matches undetermined. This is because both geometric and photometric features should be consistently similar with each other for a correct match. Introducing this partial order on matching quality to the graph-based method for range image registration allows us to find as large consistent matching with given data among all possible matches. The maximum SSK algorithm enables us to uniquely determine the largest consistent matching of points with guaranteeing the global solution. This indicates that our proposed method is useful for coarse registration.

2 Multiple Features for Reducing Matching Ambiguity

2.1 3D Point Matching Problem

A range image is defined as a set of discretely measured 3D points of an object surface where each point is represented by the coordinate system depending on a viewpoint and its orientation. Let $\boldsymbol{x}_k^i$ be the coordinates of the k-th point in the i-th image ($i = 1, 2$). We assume in this paper that RGB values $\boldsymbol{r}_k^i$ of the point (with coordinates $\boldsymbol{x}_k^i$) is also measured.

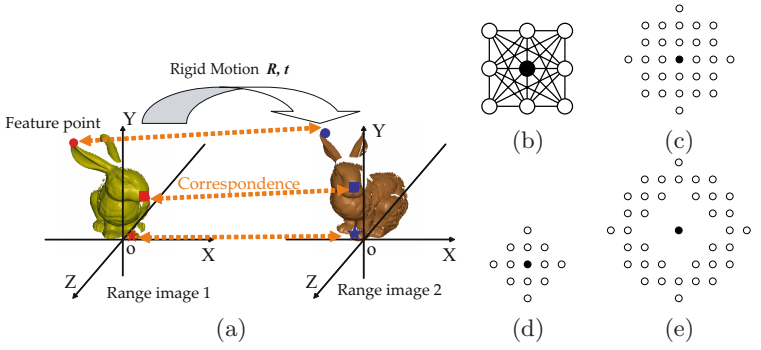

Fig. 1. Point-based registration of two range images (a) and augmented triangular mesh over 3×3 vertex neighborhood. (b) 24 elementary triangles sharing the central vertex. (c) local surface vertices neighborhood used to estimate a local normal vector from 332 triangles. (d) neighborhood for computing the triple and photometric features (52 vertices). (e) neighborhood for computing the triple feature (604 triangles).

Two coordinate systems representing two given range images are related with each other by a rigid transformation $(\boldsymbol{R}, \boldsymbol{t})$, where $\boldsymbol{R}$ is a rotation matrix and $\boldsymbol{t}$ is a translation vector. If two measured points, $\boldsymbol{x}_k^1$ and $\boldsymbol{x}_{k'}^2$, are the same point (namely, corresponding), then $\boldsymbol{x}_{k'}^2 = \boldsymbol{R}\boldsymbol{x}_k^1 + \boldsymbol{t}$. The range image registration is to find $(\boldsymbol{R}, \boldsymbol{t})$ using the corresponding points (Fig.1 (a)).

Searching for corresponding points is realized by comparing features between measured points. If two points are corresponding, then invariant features against rigid transformations should be equivalent with each other. In addition, geometric concordance should be preserved over all corresponding points, which can be evaluated by covariant features.

Some cases exist where an object shape is too smooth to discriminate measured points and thus geometric features alone do not work for reducing ambiguity in finding matching. We, therefore, employ photometric features in addition to geometric features to achieve robust registration.

2.2 Employed Features for Registration

The features we will use are computed from the augmented triangular mesh [11] which includes all possible triangles among triples of vertices in a small vertex neighborhood (Fig.1 (b)). We have chosen four local features, three of which are geometric and the other is photometric: (A) oriented surface normal, (B) structure matrix, (C) triple feature, and (D) chromaticity. We note that (A) and (B) are covariant features whereas (C) and (D) are invariant.

(A) Oriented surface normal. For each measured point $\boldsymbol{x}_k^i$, we compute its oriented surface normal $\boldsymbol{n}_k^i$ as the average over the oriented surface normals of neighboring triangles. In our experiments, we used the augmented triangular mesh over 7×7 neighborhood as shown in Fig.1 (c). We remark that these computed $\boldsymbol{n}_k^i$'s are used for computing structure matrix $\boldsymbol{S}_k^i$ and triple feature F_k^i.

(B) Structure matrix. A set of surface normals $\boldsymbol{n}_j$'s gives 3×3 structure matrix $\boldsymbol{S} = \sum_j \boldsymbol{n}_j \boldsymbol{n}_j^\top$ [11]. In our experiments, we used the augmented triangular mesh over 7×7 neighborhood as shown in Fig.1 (c).

When $\boldsymbol{x}_k^1$ and $\boldsymbol{x}_{k'}^2$ are corresponding, their structure matrices, $\boldsymbol{S}_k^1$ and $\boldsymbol{S}_{k'}^2$, satisfy $\boldsymbol{S}_{k'}^2 = \boldsymbol{R}\boldsymbol{S}_k^1\boldsymbol{R}^\top$. Letting their SVD be $\boldsymbol{S}_k^1 = \boldsymbol{U}\boldsymbol{D}\boldsymbol{U}^\top$ and $\boldsymbol{S}_{k'}^2 = \boldsymbol{U}'\boldsymbol{D}'(\boldsymbol{U}')^\top$, we have two conditions:

$$\boldsymbol{U}'\boldsymbol{P} = \boldsymbol{R}\boldsymbol{U}, \boldsymbol{D}' = \boldsymbol{D}, \tag{1}$$

where $\boldsymbol{P}$ is the 3×3 diagonal matrix $\boldsymbol{P} = \mathrm{diag}(s_1, s_2, s_1 \cdot s_2)$ $(|s_1| = |s_2| = 1)$ representing ambiguity in signs. We use this relationship to evaluate geometric concordance of transformations over corresponding points.

(C) Triple feature. Given a surface as an augmented triangular mesh, the triple feature $F_k^i = \{f_k^i(\ell), \ell = 1, 2, \ldots, t\}$ at point $\boldsymbol{x}_k^i$ represents its neighboring convexity/concavity and is defined by

$$f_k^i(\ell) = \frac{\det[\boldsymbol{n}_k^i, \boldsymbol{n}_{\Delta_1^k(\ell)}^i, \boldsymbol{n}_{\Delta_2^k(\ell)}^i]}{\|(\boldsymbol{x}_{\Delta_1^k(\ell)}^i - \boldsymbol{x}_k^i) \times (\boldsymbol{x}_{\Delta_2^k(\ell)}^i - \boldsymbol{x}_k^i)\|}, \tag{2}$$

where three vertices of the ℓ-th triangle are $\boldsymbol{x}_k^i$, $\boldsymbol{x}_{\Delta_1^k(\ell)}^i$, $\boldsymbol{x}_{\Delta_2^k(\ell)}^i$ and their oriented normal vectors are $\boldsymbol{n}_k^i$, $\boldsymbol{n}_{\Delta_1^k(\ell)}^i$, $\boldsymbol{n}_{\Delta_2^k(\ell)}^i$.

In our experiments, we computed $F_k^i[j]$ $(j = 1, 2)$ using two augmented triangular meshes (see Fig.1 (d), (e)). In our case, $t = 52$ for $j = 1$, while $t = 604$ for $j = 2$.

(D) Chromaticity. Photometric features are useful for robust registration. In particular, when an object has smooth surfaces or similar surfaces in shape, geometric features are not sufficiently discriminative while photometric features are sometimes discriminative.

In our method, as a photometric feature, we consider color distribution over neighboring points. Since RGB values themselves are sensitive to illumination conditions, we employ chromaticity which eliminates the luminance from color information.

Letting $\boldsymbol{r}_k^i$, $\boldsymbol{r}_{\Delta_1^k(\ell)}^i$, $\boldsymbol{r}_{\Delta_2^k(\ell)}^i$ be RGB values respectively at measured points $\boldsymbol{x}_k^i$, $\boldsymbol{x}_{\Delta_1^k(\ell)}^i$, $\boldsymbol{x}_{\Delta_2^k(\ell)}^i$, and $\bar{\boldsymbol{r}} = \frac{\boldsymbol{r}}{\|\boldsymbol{r}\|}$, we compute, for a measured point $\boldsymbol{x}_k^i$,

$$c_k^i(\ell)[j] = \frac{\bar{\boldsymbol{r}}_k^i[j] + \bar{\boldsymbol{r}}_{\Delta_1^k(\ell)}^i[j] + \bar{\boldsymbol{r}}_{\Delta_2^k(\ell)}^i[j]}{3}, \tag{3}$$

where $\boldsymbol{r}_k^i[j]$ is the j-th entry of $\boldsymbol{r}_k^i$ $(j = 1, 2, 3)$. We then define chromaticity distribution over neighborhood $C_k^i[j] = \{c_k^i(\ell)[j], \ell = 1, \ldots, t\}$ $(j = 1, 2, 3)$.

In our experiments, we used the augmented triangular mesh of Fig.1 (d) and thus $t = 52$ in this case.

2.3 Distribution Based Similarity Evaluation

In our method, our employed triple feature and chromaticity are computed over neighboring points and, therefore, they are defined as collections of computed

values. The Kolmogorov-Smirnov distance (KS distance) [3] enables us to compute the similarity between two collections[2]. For given triple features $F_k^1[j]$ and $F_\ell^2[j]$, the similarity $c_F(\boldsymbol{x}_k^1, \boldsymbol{x}_\ell^2)$ of the triple feature between them is defined by

$$c_F(\boldsymbol{x}_k^1, \boldsymbol{x}_\ell^2) = \prod_{j=1}^{2} \left(1 - \mathrm{KS}\left(F_k^1[j],\, F_\ell^2[j]\right)\right), \tag{4}$$

where $\mathrm{KS}\left(F_k^1[j],\, F_\ell^2[j]\right)$ represents the KS distance between $F_k^1[j]$ and $F_\ell^2[j]$. In the same way, we define the similarity $c_C(\boldsymbol{x}_k^1, \boldsymbol{x}_\ell^2)$ of chromaticity by

$$c_C(\boldsymbol{x}_k^1, \boldsymbol{x}_\ell^2) = \prod_{j=1}^{3} \left(1 - \mathrm{KS}\left(C_k^1[j],\, C_\ell^2[j]\right)\right). \tag{5}$$

3 Graph-Based Registration Method Using Multiple Features

We now extend the graph-based method [11] so that it can handle multiple features within the same framework. The graph-based matching method [11] selects as many consistent matches in best agreement with data as possible among all possible matches. In line with this idea, we formalize the range image registration problem using both geometric and photometric features in a graph. We note that our method is distinguished from existing methods in the sense that each employed feature is independently evaluated only to determine the matching-quality order and that the obtained order allows us to combinatorially determine the best matching.

3.1 Generating an Unoriented Graph $\mathcal{G}$

Along with [11], we first create an unoriented graph $\mathcal{G}$ representing uniqueness constraint of matching and geometric concordance constraint of the rigid transformation. In evaluating geometric concordance constraint, we use covariant features.

The vertex set P of $\mathcal{G}$ is defined as all putative correspondences $p = (\boldsymbol{x}_k^1,\, \boldsymbol{x}_\ell^2)$. We remark that, in the case where a search range of rigid transformations is known in advance, we can restrict putative correspondences further using our covariant feature evaluation.

The edge set E represents uniqueness of matching and geometric concordance of transformations. Namely, two vertices (i.e., two pairs of matches) are joined if they cannot occur in a matching simultaneously or if no rigid transformation exists that realizes the two pairs of matches simultaneously.

[2] The choice of the KS distance as a similarity measure in fact allows us to combine our triple feature and chromaticity by computing the product of c_F and c_C in Eqs. (4) and (5). It should be stressed, however, that our approach is general and does work for any other similarity measures and their combination.

3.2 Generating an Oriented Graph $\mathcal{D}$

It should be clear that if $M \subset P$ is a solution of the matching problem, no pair of entries in M should be connected by any edge in $\mathcal{G}$. In other words, every possible matching M is an independent vertex subset of $\mathcal{G}$. Since many independent vertex subsets exist in $\mathcal{G}$, we, therefore, select the one that is in best agreement with data.

To do so, we here add orientations to the edges of $\mathcal{G}$ to create oriented graph $\mathcal{D}$ where we evaluate invariant features to determine the orientation of an edge. In this evaluation, [11] uses a single feature alone while our method employs multiple features.

For a putative correspondence $p = (\boldsymbol{x}_k^1, \boldsymbol{x}_\ell^2) \in P$, we denote by $\boldsymbol{c}(p)$ the 2D vector whose entries are the similarities of the triple feature and chromaticity, respectively. Based on $\boldsymbol{c}(\cdot)$, we give the orientation to each edge in $\mathcal{G}$ to define $\mathcal{D} = (P, A \cup A^*)$. Here, A and A^* represent bidirectional edges and unidirectional edges, respectively. We note that $A \cap A^* = \emptyset$.

For two pairs of matches, $p, q \in P$, if $\boldsymbol{c}(p) - \boldsymbol{c}(q)$ is positive for all entries of $\boldsymbol{c}(\cdot)$, then let $(q, p) \in A^*$ (i.e., an oriented edge from q to p). Inversely, if $\boldsymbol{c}(p) - \boldsymbol{c}(q)$ is negative for all entries of $\boldsymbol{c}(\cdot)$, then let $(p, q) \in A^*$. Otherwise, we define $(p, q), (q, p) \in A$. We remark here that we can incorporate robustness further by testing if $\boldsymbol{c}(p) - \boldsymbol{c}(q) > t$, where t is a small positive constant.

3.3 Strict Sub-kernel of $\mathcal{D}$

The maximum matching we are looking for is identical with the maximum strict sub-kernel (SSK in short) [10] of oriented graph $\mathcal{D} = (P, A \cup A^*)$ defined above. We remind that the SSK, $K \subseteq P$, of $\mathcal{D}$ is an independent vertex subset in $\mathcal{D}$ and that, for any $p \in K$, the existence of $r \in K$ is ensured such that $(q, r) \in A^*$ for every $(p, q) \in A \cup A^*$. Uniqueness of the SSK in $\mathcal{D}$ is guaranteed and an polynomial algorithm for finding the SSK is known [9,10,11].

Finally we summarize the characteristics of our approach. First, for each feature, similarity between two points is independently evaluated. In other words, for two pairs of matches, each feature independently gives the matching-quality order only and our method focuses on the combination of matches based on this order. Differently from other existing methods, our method does not either define any single metric for similarity using multiple features or minimize any cost function derived from employed features. Secondly, employing geometric features as well as photometric features in the graph-based method enhances robustness in registration. If an object has insufficiently discriminative surfaces in shape, the SSK using geometric features alone may find incorrect matching because two points locally having similar shapes happen to generate the SSK. In contrast, incorporating evaluation of photometric features as well leads to excluding the possibility of generating the SSK that includes such points. Accordingly, ambiguities in matching are reduced and robust registration is achieved. This can be also understood from the fact that points included in the SSK have to be superior in both geometric and photometric similarities to all competing points.

4 Range Image Registration Using SSK

4.1 Interest Point Detection

We detect interest points using triple features among measured points. For each measured point $\boldsymbol{x}_k^i$, we compute the standard deviation of triple features over its neighborhood[3]: $L_k^i = \mathrm{std} \bigcup_{j=1}^{r} F_k^i(j)$. L_k^i becomes large for a point whose neighboring surface shape is not uniform. We thus detect points with local maxima of L_k^i. We call them interest points in this paper.

Then, we use two sets of interest points, each of which is independently detected from one of two given range images, and generate a table for all possible matches. In generating the table, we eliminate matches that do not satisfy a given search range of rigid transformations. To be more concrete, for a given corresponding pair of points, we compute their structure matrices and then decompose them using SVD to find the rotation relating the pair (cf. Eq. (1)). Next, we eliminate the pair from the table if the rotation is not admissible.

4.2 Maximum SSK and Matching

Based on the generated table, we consider all possible matches and then define the vertex set of unoriented graph $\mathcal{G}$. We then define edges along with uniqueness of matching and geometric concordance. Next we give the orientation to the edges in $\mathcal{G}$ using Eqs. (4) and (5).

As a result, we obtain oriented graph $\mathcal{D}$ representing our problem. The SSK algorithm uniquely finds the best matching in $\mathcal{D}$ [11].

5 Experiments

To demonstrate the potential applicability of the proposed method, we applied our method to synthetic range images.

We used a horse model provided by [17] and attached randomly generated texture to it in order to generate its range images (Fig. 2). The body of the horse model was scanned at 20 degree rotation steps with respect to the Y-coordinate and 18 range images with the size of 200×200 pixels were obtained. We then perturbed the Z-coordinate of each point in the range images by adding Gaussian noise with zero mean and standard deviation of $\sigma = 0.1$. This implies that if the height of the horse body is about 60cm, the added noise is about 1mm.

We applied our method to all adjacent pairs in the range image sequence above. We set the search range of ration angles be $\pm 15^\circ$ different from the ground truths just for reducing computational cost. We remark that we did not have any assumption about the rotation axis to be found. To see the effectiveness of our method, we also applied a method using geometric features alone to the same data. The registration results are shown in Fig. 3 and Table 1. Fig. 3 presents selected interest points and their matches obtained by the two methods.

[3] $F_k^i(1)$ and $F_k^i(2)$ are computed with Eq. (2) over 52 and 604 triangles respectively, as shown in Fig. 1 (d), (e). L_k^i is standard deviation over them.

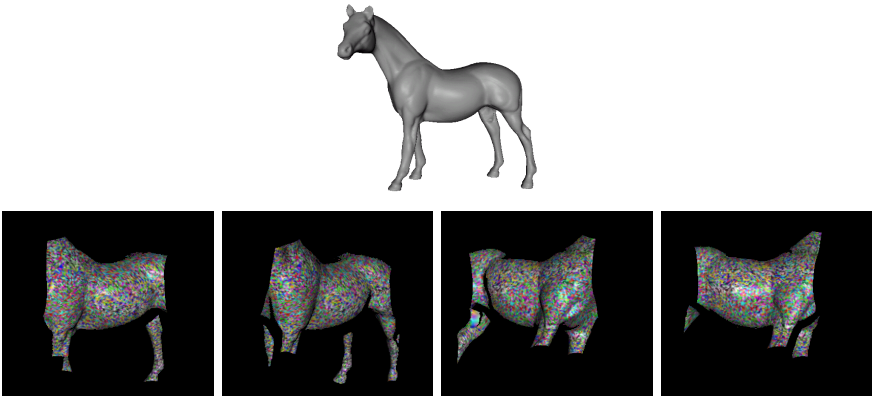

Fig. 2. Horse model and its synthetic range images

Table 1. Evaluation of registration results ("−" means failure in estimation)

	i	1	2	3	4	5	6	7	8	9
	points	11616	10888	9913	9374	9442	9778	10503	11589	12118
	IPs of i-th image	173	241	210	173	197	210	260	178	172
	IPs of $(i+1)$-th image	237	229	172	193	269	243	190	171	172
shape and color	matches	11	5	7	7	8	11	9	7	9
	estimated rotation [°]	20.1	21.1	16.6	19.9	20.1	19.9	20.1	20.2	20.0
	rotation error [°]	0.2	1.0	5.5	0.3	0.8	0.2	1.2	0.3	0.3
	translation error	0.2	1.5	4.4	0.1	0.2	0.1	0.4	0.2	0.2
shape only	matches	3	13	11	11	9	13	10	17	4
	estimated rotation [°]	46.9	19.7	35.2	24.8	15.8	21.1	20.4	19.9	-168.9
	rotation error [°]	63.1	1.7	14.6	19.6	17.2	6.8	11.6	0.2	71.5
	translation error	29.2	0.4	20.2	7.3	21.9	1.4	1.4	0.2	21.2

	i	10	11	12	13	14	15	16	17	18
	Points	11929	11464	10735	9779	8957	9198	10105	11228	11725
	IPs of i-th image	179	256	302	331	250	178	145	166	135
	IPs of $(i+1)$-th image	225	285	328	307	154	140	165	153	156
shape and color	matches	3	2	7	12	2	3	8	5	10
	estimated rotation [°]	19.9	-	19.6	19.8	-	19.9	19.9	20.0	20.1
	rotation error [°]	1.1	-	1.2	0.3	-	2.2	0.8	1.0	0.1
	translation error	0.1	-	0.6	0.3	-	0.8	0.1	0.6	0.0
shape only	matches	2	3	15	10	12	5	17	4	21
	estimated rotation[°]	-	16.2	15.8	43.4	24.5	11.9	19.5	23.4	19.4
	rotation error [°]	-	71.5	18.7	67.4	8.4	38.1	2.1	30.9	3.6
	translation error	-	38.9	7.1	40.8	8.5	19.9	0.6	10.7	1.3

In Table 1, the i-th column corresponds to the registration result of the i-th and $(i+1)$-th images. The number of measured points, the number of detected interest points (IPs), the number of obtained matches (the number of vertices in the obtained SSK), the estimated rotation angle, error of the estimated rotation axes, and translation error are presented there. Errors of the estimated rotation axes were evaluated by the difference from the ground truth while translation errors were by the difference between norms. Since the rigid transformation was estimated using the 3D coordinates of matched points [15], we need at least three matches. "−" was used in the case of less than three matches, which means failure in estimation.

Table 1 shows that over all the cases, the registration accuracy of our method is not only significantly higher but also numerically more stable, compared with the method using geometric features alone. In fact, in our method, errors of

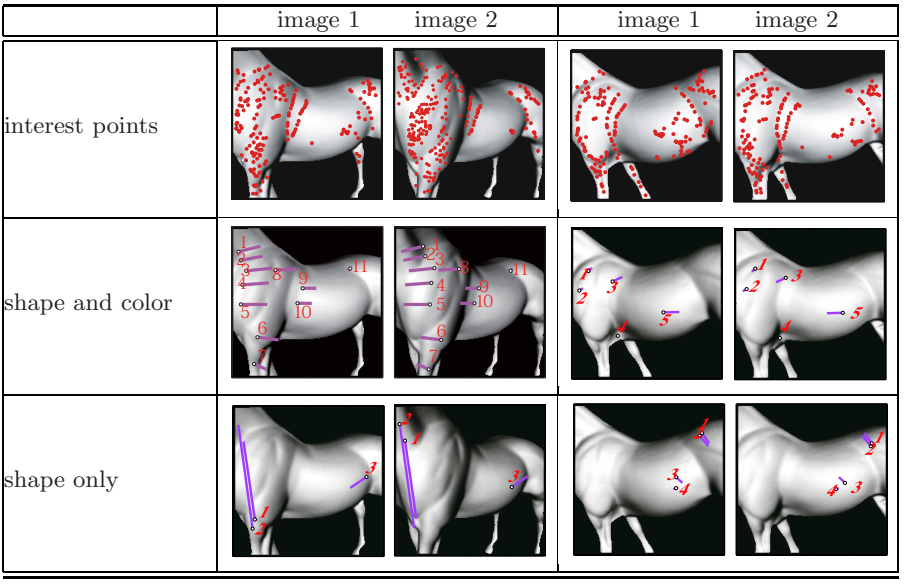

Fig. 3. Examples of registration results

estimated rotations were within ±1 degree and translation errors were within 1.0 except for two cases failing in estimation. These observations can be understood by the fact that discriminative geometric features are not expected due to smoothness of the shape of the horse body while photometric features are discriminative even for such shapes in this case. Fig. 3 certificates this because vectors connecting matched feature points have the uniform direction in our method while they do not in the case of geometric features alone. Similarity derived from our photometric feature reduces matching ambiguity using geometric features alone and matching-quality of incorrect matches as well, which prevents such matches from being included in the SSK. Here we remark again that we did not assume any rotation axis to be found; this suffices to show that our proposed method, differently from existing methods, does not require any good initial estimation. We can thus conclude that our method achieves sufficiently accurate registration without any good initial estimation.

6 Conclusion

We extended a graph-based range image registration method so that it can handle both geometric and photometric features simultaneously. Namely, we formulated registration as a graph-based optimization problem where we independently evaluate geometric feature and photometric feature and then consider only the order of point-to-point matching quality. We then find as large consistent matching as possible in the sense of the matching-quality order. This is solved as one global combinatorial optimization problem of polynomial complexity. The advantage of our method is that each match is independently evaluated

by each employed feature and the order of matching-quality is only concerned. Differently from existing methods, our proposed method need not define any single metric of similarity for evaluating matching. Our experimental results demonstrate the effectiveness of our method for coarse registration.

The proposed method will reduce the possibility of finding an incorrect matching but cannot be expected to increase the number of matches significantly. This follows from the fact that both the two similarity criteria have to be consistent. In principle, it is also possible to combine the two criteria in such a way that when one of them strictly favors the match of q to p and the other is at least indifferent between p and q, the edge joining p and q becomes unidirectional. Such definition requires using a different matching algorithm from the one used in this paper. This research direction is our ongoing work.

Acknowledgments. A part of this work was done under the framework of MOU between the Czech Technical University and National Institute of Informactics. This work is in part supported by the Czech Academy of Sciences under project 1ET101210406 and by the EC project MRTN-CT-2004-005439.

References

1. Besl, P.J., McKay, N.D.: A Method for Registration of 3-D Shapes. IEEE Trans. on PAMI 14(2), 239–256 (1992)
2. Chen, Y., Medioni, G.: Object Modeling by Registration of Multiple Range Images. IVC 10(3), 145–155 (1992)
3. Duda, R.O., Hart, P.E., Stork, D.G.: Pattern Classification, 2nd edn. John Willey and Sons, Inc. New York (2001)
4. Feldmar, J., Ayache, N., Berring, F.: Rigid, Affine and Locally Affine Registration of Free-Form Surfaces. IJCV 18(2), 99–119 (1996)
5. Godin, G., Laurendeau, D., Bergevin, R.: A Method for the Registration of Attributed Range Images, Proc. of 3DIM, pp. 179–186 (2001)
6. Guest, E., Berry, E., Baldock, R.A., Fidrich, M., Smith, M.A.: Robust Point Correspondence Applied to Two and Three-Dimensional Image Registration. IEEE Trans. on PAMI 23(2), 165–179 (2001)
7. Okatani, I.S., Sugimoto, A.: Registration of Range Images that Preserves Local Surface Structures and Color, Proc. 3DPVT, pp. 786–796 (2004)
8. Rusinkiewicz, S., Levoy, M.: Efficient Variants of the ICP Algorithm, Proc. of 3DIM, pp. 145–152 (2001)
9. Šára, R.: Finding the largest unambiguous component of stereo matching. In: Heyden, A., Sparr, G., Nielsen, M., Johansen, P. (eds.) ECCV 2002. LNCS, vol. 2352, pp. 900–914. Springer, Heidelberg (2002)
10. Šára, R.: Robust Correspondence Recognition for Computer Vision. In: Proc. of 17th ERS-IASC Symposium on Computational Statistics, pp. 119–131 (2006)
11. Šára, R., Okatani, I.S., Sugimoto, A.: Globally Convergent Range Image Registration by Graph Kernel Algorithm, Proc. of 3DIM, pp. 377–384 (2005)
12. Sharp, G.C., Lee, S.W., Wehe, D.K.: ICP Registration Using Invariant Features. IEEE Trans. on PAMI 24(1), 90–102 (2002)
13. Silva, L., Bellon, O.R.P., Boyer, K.L.: Enhanced, Robust Genetic Algorithms for Multiview Range Image Registration, Proc. of 3DIM, pp. 268–275 (2003)

14. Turk, G., Levoy, M.: Zipped Polygon Meshes from Range Images, ACM SIGGRAPH Computer Graphics, pp. 311–318 (1994)
15. Umeyama, S.: Least-Square Estimation of Transformation Parameters Between Two Point Patterns. IEEE Trans. on PAMI 13(4), 376–380 (1991)
16. Zhang, Z.: Iterative Point Matching for Registration of Free-Form Curves and Surfaces. IJCV 13(2), 119–152 (1994)
17. Georgia Institute of Technology Large Geometric Models Archive `http://www-static.cc.gatech.edu/projects/large_models/`